



10 **Abstract**

11 Degraded water quality in rivers and streams can have large economic, societal and ecological impacts.
12 Stream water quality can be highly variable both over space and time. To develop effective management
13 strategies for riverine water quality, it is critical to be able to predict these spatio-temporal variabilities.
14 However, our current capacity to model stream water quality is limited, particularly at large spatial
15 scales across multiple catchments. This is due to a lack of understanding of the key controls that drive
16 spatio-temporal variabilities of stream water quality. To address this, we developed a Bayesian
17 hierarchical statistical model to analyse the spatio-temporal variability in stream water quality across
18 the state of Victoria, Australia. The model was developed based on monthly water quality monitoring
19 data collected at 102 sites over 21 years. The modelling focused on six key water quality constituents:
20 total suspended solids (TSS), total phosphorus (TP), filterable reactive phosphorus (FRP), total Kjeldahl
21 nitrogen (TKN), nitrate-nitrite (NO_x), and electrical conductivity (EC). Among the six constituents, the
22 models explained varying proportions of variation in water quality. EC was the most predictable
23 constituent (88.6% variability explained) and FRP had the lowest predictive performance (19.9%
24 variability explained). The models were validated for multiple sets of calibration/validation sites and
25 showed robust performance. Temporal validation revealed a systematic change in the TSS model
26 performance across most catchments since an extended drought period in the study region, highlighting
27 potential shifts in TSS dynamics over the drought. Further improvements in model performance need to
28 focus on: (1) alternative statistical model structures to improve fitting for the low concentration data,
29 especially records below the detection limit; and (2) better representation of non-conservative
30 constituents by accounting for important biogeochemical processes. We also recommend future
31 improvements in water quality monitoring programs which can potentially enhance the model capacity,
32 via: 1) improving the monitoring and assimilation of high-frequency water quality data; and 2)
33 improving the availability of data to capture land use and management changes over time.

34 **Keywords**

35 stream water quality; spatio-temporal variability; sediments; nutrients; statistical modeling; Bayesian
36 hierarchical model



37 **1. Introduction**

38 Deteriorating water quality in aquatic systems such as rivers and streams can have significant
39 environmental, economic and social ramifications (e.g. Whitworth et al., 2012;Vörösmarty et al.,
40 2010;Qin et al., 2010;Kingsford et al., 2011). However, our ability to manage and mitigate water quality
41 impacts is hampered by the variability in water quality both across space and time, and our inability to
42 predict this variability (Chang, 2008;Bengraïne and Marhaba, 2003;Ai et al., 2015). Water quality
43 conditions can vary across individual events, as well as at daily, seasonal and inter-annual scales at an
44 individual location (Arheimer and Lidén, 2000; Kirchner et al., 2004; Larned et al., 2004; Pellerin et al.,
45 2012; Saraceno et al., 2009). Water quality conditions also typically differ significantly across locations
46 (Meybeck and Helmer, 1989). These variabilities in stream water quality are driven by three key
47 mechanisms: (1) the source of constituents, which defines the total amount of constituents being
48 available in a catchment; (2) the mobilization of constituents in particulate and dissolved forms, which
49 detaches constituents from their sources via processes such as erosion and biogeochemical processing;
50 and (3) the delivery of mobilized constituents from catchments to receiving waters via multiple
51 hydrologic pathways including surface and subsurface flow (Granger et al., 2010).

52 Spatial variability in stream water quality is driven by natural catchment characteristics (e.g., climate,
53 geology, soil type, topography and hydrology) as well as by human activities within catchments (e.g.,
54 land use and management, vegetation cover etc.), all of which control the extent and magnitude of the
55 three key mechanisms described above (Lintern et al., 2018a). At the same time, temporal shifts in water
56 quality are influenced by changes in climatic, hydrological and other catchment conditions, such as
57 temperature (Roberts and Mulholland, 2007), the timing and magnitude of rainfall events (Fraser et al.,
58 1999), runoff generation and streamflow (Ahearn et al., 2004; Mellander et al., 2015; Sharpley et al.,
59 2002), and vegetation cover changes over time (Kaushal et al., 2014;Ouyang et al., 2010).

60 Despite understanding of the basic mechanisms, we currently lack the ability to model these spatio-
61 temporal variabilities at larger scales to inform the development of effective policy and mitigation
62 strategies. Conceptual or physically-based water quality models are typically limited by the
63 simplification of physical processes (Hrachowitz et al., 2016). Furthermore, practical implementation
64 of these models can be also limited by the intensive requirements of data and calibration effort,



65 particularly for large regions with varying catchment conditions (Fu et al., 2018; Abbaspour et al., 2015).
66 In contrast, whilst most statistical water quality models are easier to implement, they often focus on
67 either the spatial variation of time-averaged water quality conditions (Tramblay et al., 2010; Ai et al.,
68 2015), or the temporal variation at individual locations (Kisi and Parmar, 2016; Kurunç et al.,
69 2005; Parmar and Bhardwaj, 2015). Consequently, it remains challenging to address spatio-temporal
70 variability simultaneously over long time periods and large regions. This lack of integrated modelling of
71 both spatial and temporal variability in water quality can not only limit our understanding of the key
72 factors that affect water quality dynamics over both of these dimensions. It also hinders our ability to
73 predict future water quality changes in un-monitored locations.

74 The aim of this research is to develop a data-driven model to predict spatio-temporal changes in stream
75 water quality. This model was established using long-term (21 years) stream water quality observations
76 across 102 catchments in the state of Victoria, Australia. The model built on two previous studies on the
77 same dataset that identified the key drivers for water quality spatial and temporal variabilities,
78 respectively (Lintern et al., 2018b; Guo et al., 2019). Our approach aims to bridge the gap between fully-
79 distributed water quality models and statistical approaches to provide useful information for catchment
80 managers, especially for large-scale water quality assessments.

81 **2. Method**

82 **2.1 Spatio-temporal modelling framework**

83 A Bayesian hierarchical approach was used to model the spatio-temporal variability in stream water
84 quality. The Bayesian approach enables the inherent natural stochasticity of water quality to be
85 incorporated into the model (Clark, 2005), and the hierarchical model structure enables the key controls
86 of temporal variability in water quality to vary across locations (Webb and King, 2009; Borsuk et al.,
87 2001).

88 The structure of this model is presented below in Eq. 1 to 6. The transformed concentration of a
89 constituent (see Sect. 2.2 for justification) at time i and site j (C_{ij}) is assumed to be normally distributed
90 with a mean μ_{ij} and standard deviation σ representing inherent randomness (Eq. 1).

$$C_{ij} \sim N(\mu_{ij}, \sigma) \quad (1)$$



91 To represent spatio-temporal variability, μ_{ij} is modelled as the sum of the site-level mean constituent
92 concentration (\bar{C}_j) and the deviation from that mean at time i (Δ_{ij}) (Eq. 2).

$$\mu_{ij} = \bar{C}_j + \Delta_{ij} \quad (2)$$

93 To describe spatial variability, the site-level mean (\bar{C}_j) is modelled as a linear function of a global
94 intercept (int), and the sum of the m catchment characteristics $S_{1,j}$ to $S_{m,j}$ (e.g. land use, topography)
95 weighted by their relative contributions to spatial variability (β_{S_1} to β_{S_m}) (Eq. 3).

$$\bar{C}_j = int + \beta_{S_1} \times S_{1,j} + \beta_{S_2} \times S_{2,j} + \dots + \beta_{S_m} \times S_{m,j} \quad (3)$$

96 The temporal variability, represented by the deviation from the mean (Δ_{ij}), is a linear combination of n
97 temporal variables, $T_{1,ij}$ to $T_{n,ij}$ (e.g., climate condition, streamflow, vegetation cover) (Eq. 4), at time
98 i and site j .

$$\Delta_{ij} = \beta_{T_1} \times T_{1,ij} + \dots + \beta_{T_n} \times T_{n,ij} \quad (4)$$

99 To account for differences in these temporal influences across sites, the effect of each temporal variable
100 at site j ($\beta_{T_N,j}$ with N in 1,2, ... n) is drawn from a distribution with a mean of $N_{\beta_{T_N,j}}$ (Eq. 5), which
101 is then modelled with a linear combination of two additional catchment characteristics, $S_{TN1,j}$ and
102 $S_{TN2,j}$ (Eq. 6).

$$\beta_{T_N,j} \sim N(\mu_{\beta_{T_N,j}}, \sigma_{\beta_{T_N,j}}), \text{ for } N \text{ in } 1, 2, \dots \quad (5)$$

$$N_{\beta_{T_N,j}} = int_{\beta_{TN}} + \beta_{S_{TN1}} \times S_{TN1,j} + \beta_{S_{TN2}} \times S_{TN2,j} \quad (6)$$

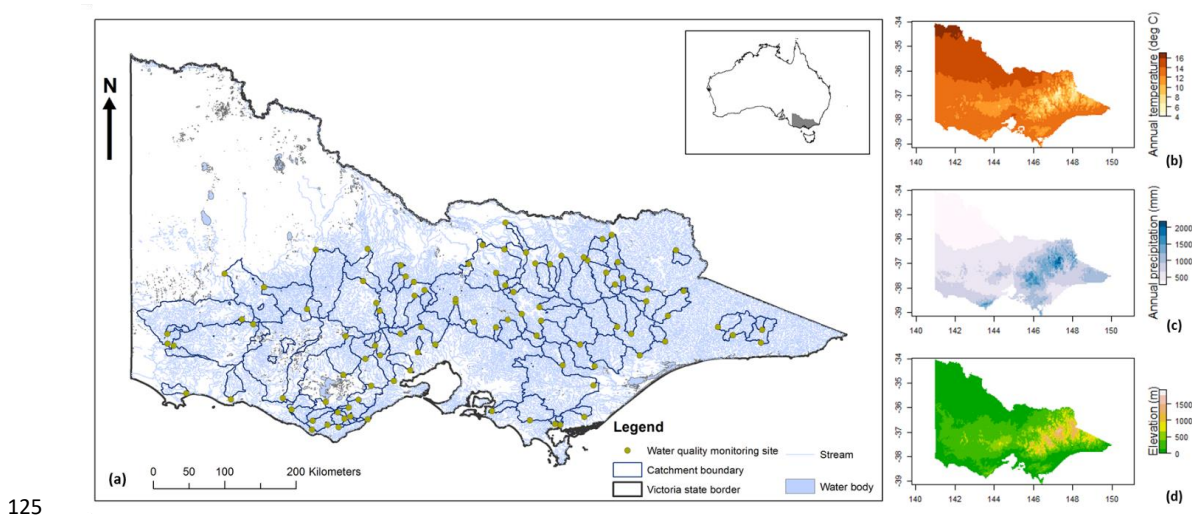
103 Section 2.2 introduces the data used to develop these Bayesian hierarchical models. Section 2.3
104 describes how the detailed model structure was determined, including the choice of key predictors for
105 the spatial variability (i.e., catchment characteristics $S_{1,j}$ to $S_{m,j}$) and temporal variability (i.e. $T_{1,ij}$ to
106 $T_{n,ij}$ and $S_{TN1,j}$ and $S_{TN2,j}$), and all their corresponding coefficient values. The approaches to evaluate
107 model performance and robustness are described in Sect. 2.4.

108 2.2 Data collection and processing

109 The Bayesian hierarchical models were developed with 21-year stream water quality observations at
110 102 catchments in state of Victoria, Australia. The collection and processing of the data are detailed in
111 previous publications that worked with the same dataset (Lintern et al., 2018b; Guo et al., 2019). Briefly,



122 however, stream water quality data were extracted from the Victorian Water Measurement Information
123 System (Department of Environment Land Water and Planning Victoria, 2016b), which contains
124 monthly grab samples of water quality at approximately 400 sites across Victoria. Water quality data
125 sampled between 1994 and 2014 at 102 sites were used to develop the model (Fig. 1). This was because
126 these sites and this time period provided the longest consistent period of continuous records over the
127 greatest number of monitoring sites. The catchments corresponding to these water quality monitoring
128 sites were delineated using the Geofabric tool (Bureau of Meteorology, 2012), and have areas ranging
129 from 5 km² to 16,000 km². The water quality parameters of interest were: total suspended solids (TSS),
130 total phosphorus (TP), filterable reactive phosphorus (FRP), total Kjeldahl nitrogen (TKN), nitrate-
131 nitrite (NO_x) and electrical conductivity (EC). These parameters represent sediments, nutrients and salts,
132 which are some of the key concerns for water quality managers in Australia and around the world. These
133 water quality data were sampled following standard DELWP protocols (Australian Water Technologies,
134 1999) and analysed in National Association of Testing Authorities accredited laboratories .



125

126 **Figure 1. Map of (a) the 102 selected water quality monitoring sites and their catchment**
127 **boundaries, with insert showing the location of the state of Victoria within Australia; (b) annual**
128 **average temperature and (c) annual precipitation and (d) elevation across Victoria.**

129 We selected potential spatial explanatory variables (i.e. predictors to explain spatial variability) based
130 on catchment characteristics that are widely known to influence water quality condition (Lintern et al.,
131 2018a). Fifty potential explanatory catchment characteristics were selected based on a literature review .



132 These included catchment land use, land cover, topographic, climatic, geological, lithological and
133 hydrological catchment characteristics. These variables were derived using datasets obtained from
134 Geoscience Australia (2004, 2011), the Bureau of Meteorology (2012), the Bureau of Rural Sciences
135 (2010), Department of Environment Land Water and Planning Victoria (2016) and the Terrestrial
136 Ecosystem Research Network (2016) (see Table S1 in the Supplementary Material for detailed variable
137 names and data sources). We used a static set of land use data from 2005-2006 to represent the entire
138 study period, as a preliminary analysis of land use data between 1996 and 2011 suggested less than 1%
139 changes (i.e. agricultural, grazing, conservation).

140 Temporal explanatory variables of discharge (originally in ML d^{-1}) and water temperature ($^{\circ}\text{C}$)
141 corresponding to the same timestamps for water quality observations were also extracted for each site
142 over the study period (Department of Environment Land Water and Planning Victoria, 2016). Discharge
143 was converted to streamflow (mm d^{-1}) for each catchment, which allowed us to also calculate the average
144 streamflows over 1, 3, 7, 14 and 30 days preceding the water quality sampling dates. In addition, gridded
145 climate data (Frost et al., 2016; Raupach et al., 2009, 2012) and the normalized difference vegetation
146 index (NDVI) data (NASA LP DAAC, 2017; Eidenshink, 1992) were also extracted to calculate the
147 catchment average daily rainfall (mm), daily evapotranspiration (ET) (mm), daily average temperature
148 ($^{\circ}\text{C}$), daily root zone (shallower than 1m) and deep (deeper than 1m) soil moisture, as well as monthly
149 NDVI. A summary of these data and their sources is in Table S2 in the Supplementary Material.

150 The raw input data were filtered and transformed to increase the data symmetry, making them more
151 suitable for use in the linear spatio-temporal model structure (Eqs. 3, 4 and 6). For the filtering process,
152 we first removed all water quality records with flags of quality issues and values below the limits of
153 reporting (LOR). This was because that uncertainty of values below LOR may amplify after the
154 transformation, posing large influence in the subsequent model fitting. Furthermore, those low
155 concentrations were of less interest; poor water quality conditions (i.e., high constituent concentrations)
156 were our primary concerns to model. Water quality records corresponding to days with zero flows were
157 also excluded from further analyses.

158 For the transformation process, we transformed the data of each of the spatial catchment characteristics,



159 temporal explanatory variables, as well as each constituent to improve the symmetry of individual
160 distributions. The log-sinh transformation (Wang et al., 2012) was used for all catchment characteristics
161 due to the presence of zero values in several characteristics (e.g., percentage area of different types of
162 land use). The best log-sinh transformation parameter was determined for each spatial explanatory
163 variable across all 102 catchments. In addition, all observed constituent concentrations and temporal
164 explanatory variables were Box-Cox transformed. For each variable, i.e., 21-year time-series data across
165 all 102 sites, we first identified the optimal Box-Cox parameter at each site λ , and then the averaged λ
166 across all sites to determine the final λ used to transform a respective variable. This ensured a consistent
167 transformation for each variable across all sites. All log-sinh and Box-Cox transformation parameters
168 used are summarized in Table S3 and S4 in the Supplementary Material.

169 **2.3 Model fitting**

170 Based on the general spatio-temporal modelling structure (Eqs. 2 to 6), we identified the best spatial
171 predictors (S_1 to S_m in Eq. 3) and the best temporal predictors (T_1 to T_n in Eq. 4) in two sequential
172 studies (Lintern et al., 2018b; Guo et al., 2019). The predictors were selected using an exhaustive search
173 approach (May et al., 2011; Saft et al., 2016), which considered a large number of potential predictors
174 and all possible combinations of these predictors. This selection approach required firstly fitting an
175 individual model to each candidate predictor set, and then comparing all fitted models to select a single
176 best set of predictors. Alternative models were evaluated based on the Akaike Information Criterion
177 (AIC) (Akaike, 1974) and Bayesian Information Criterion (BIC) (Schwarz, 1978) to ensure optimal
178 balance between model performance and complexity.

179 The key factors identified for the spatial and temporal variabilities in each constituent are listed in Tables
180 S5 and S6 in the Supplementary Materials. General speaking, the key factors controlling the spatial
181 variability in river water quality were land-use and long-term climate conditions (Lintern et al., 2018b).
182 Temporal variability was mainly explained by temporal changes in streamflow conditions, water
183 temperature and soil moisture (Guo et al., 2019). We further modelled the spatial variation in each of
184 these temporal relationships (β_{T_1} to β_{T_n} in Eq. 4) with two spatial characteristics, S_{TN1} and S_{TN2} (Eq.
185 6), where a higher number of predictors was not used to avoid over-fitting. We found S_{TN1} and S_{TN2}



186 via a Spearman correlation analyses ($p < 0.05$) between the fitted parameter values of each temporal
187 predictor variable (β_{T_1} to β_{T_n}) and potential spatial explanatory variables as mentioned in Sect. 2.2.
188 S_{TN1} and S_{TN2} were selected as the two catchment characteristics which had the highest correlations
189 with the fitted parameter values of each temporal predictor, which were also summarized in Table S6 in
190 the Supplementary Material.

191 After identifying the predictors for each constituent, the Bayesian hierarchical spatio-temporal model
192 was fitted for each constituent across all monitoring sites. To achieve this, we used the R package *rstan*
193 (Stan Development Team, 2018), which enabled both the sampling of parameter values from posterior
194 distributions with Markov chain Monte Carlo (MCMC) and model evaluation. Constituent standard
195 deviation (σ) was assumed to be drawn from a prior of minimally informative distribution of half-normal
196 $N(0,10)$ that was truncated to only positive values (Gelman, 2006; Stan Development Team, 2018). The
197 regression coefficient of each spatial predictor ($\beta_{S_1}, \beta_{S_2}, \dots, \beta_{S_m}$ in Eq. 3) was assumed to be drawn
198 from an independent hyper-parameter normal distribution with mean of β_S and standard deviation of
199 σ_S . The site-level regression coefficients of the temporal predictors ($\beta_{T_{1,j}}, \beta_{T_{2,j}}, \dots, \beta_{T_{n,j}}$ in Eq. 4,
200 respectively) were sampled from the corresponding hyper-parameter normal distribution with means of
201 $\mu_{\beta_{T_1}}, \mu_{\beta_{T_2}}, \dots, \mu_{\beta_{T_n}}$ and standard deviations of $\sigma_{\beta_{T_1}}, \sigma_{\beta_{T_2}}, \dots, \sigma_{\beta_{T_n}}$. The hyper-parameters
202 were further assumed to be drawn from minimally informative normal distributions with $N(0,5)$ (for all
203 the means) and minimally informative half-normal distribution of $N(0,10)$ that was truncated to only
204 positive values (for all the standard deviations). In each model run there were four independent Markov
205 chains. A total of 20,000 iterations were used for each chain. Convergence of the chains was checked
206 using the *Rhat* value (Sturtz et al., 2005).

207 **2.4 Model performance and sensitivity analyses**

208 The performance of the fitted model for each constituent was first evaluated by comparing the simulated
209 and observed concentrations at 102 sites altogether to understand how the full spatio-temporal
210 variabilities were captured (Sect. 3.1). As explained in Sect. 2.2, the model calibration for each
211 constituent was performed with only the above-LOR data. Therefore, model performance was first
212 evaluated with only these above-LOR data. Performance was then evaluated with the full dataset
213 including the below-LOR data, to understand the model capacity to simulate the full distribution of



214 constituent concentration. In addition, the model performance for capturing spatial differences was
215 assessed by comparing the simulated and observed long-term mean concentration at each site. The
216 performance assessments were based on both visual inspection of model fitting as well as the Nash-
217 Sutcliffe efficiency (NSE), which suggested the proportion of variability that can be explained by the
218 models (Nash and Sutcliffe, 1970).

219 Additional evaluations of model sensitivity were conducted with calibration and validation on subsets
220 of the full data (Sect. 3.2). Firstly, to understand the sensitivity of the model to the monitoring sites
221 included for calibration, we randomly selected 80% of the sites for calibration and used the remaining
222 20% for validation, and repeated this validation process for five times for each constituent. The
223 calibration and validation performance was compared to each other, as well as with the performance of
224 the full model.

225 We also evaluated the model sensitivity to the periods of calibration. Since the study region was greatly
226 influenced by a prolonged drought from 1997 to 2009 - known as the Millennium Drought, we focused
227 on analysing the impact of this drought period. Specifically, we calibrated the model for each constituent
228 to pre-, during- and post-drought periods (1994-1996, 1997-2009 and 2010-2014, respectively) and then
229 validated the model on the remaining period which was not used for calibration. For example, when
230 calibrating to the pre-drought period (1994-1996), validation was performed on both the during and
231 post-drought data (1997-2014). Each corresponding calibration and validation performance was
232 compared with each other as well as against that of the full model, to identify potential impacts of the
233 drought on model robustness.

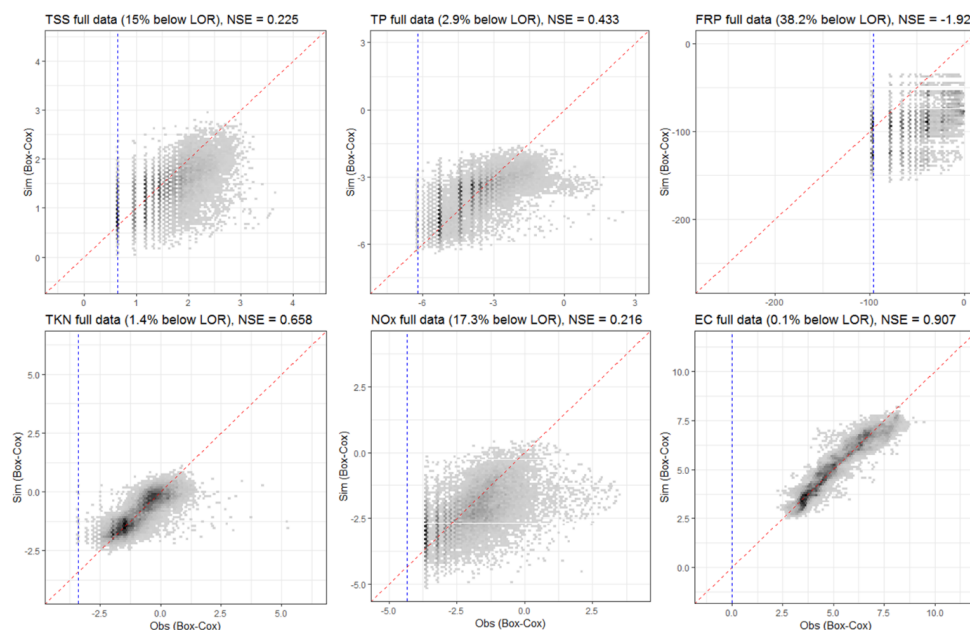
234 **3. Results**

235 **3.1 Model performance**

236 The spatio-temporal water quality models show varying performances among the constituents. When
237 assessed with only the above-LOR data (Fig. 2), the best performing models are those for EC and TKN,
238 which capture 90.7% and 65.8% of the total observed spatio-temporal variability. The modelling power
239 is lowest for FRP (NSE = -1.92), which might be related to the large number of FRP records below the
240 LOR (38%). Similar to FRP, poorer model performance is also observed for NO_x and TSS, with NSE



241 values of 0.216 and 0.225, where the proportion of below-LOR samples were 17.3% and 15%,
 242 respectively. When evaluated against the entire dataset (i.e., including both below- and above LOR
 243 data), the models explain 19.9% (FRP) to 88.6% (EC) of spatio-temporal variability (Table 1). Model
 244 performances for FRP, NO_x and TSS improve notably compared with previous evaluation on above-
 245 LOR data. However, FRP, NO_x and TSS remain as the three constituents that are most difficult to
 246 predict. We further discuss the possible factors influencing their model performance in Sect. 4.2.



247

248 **Figure 2. Performance of the spatio-temporal models for each of the six constituents,**
 249 **represented by the simulated and observed concentrations of above-LOR records across all 102**
 250 **calibration sites, in Box-Cox transformed space. Darker regions represent denser distribution of**
 251 **simulation and observation points. Dashed red lines show the 1:1 lines whereas dashed blue lines**
 252 **show the LOR levels. For each constituent, the percentage of data below the LOR and the model**
 253 **performance (NSE) are also specified.**

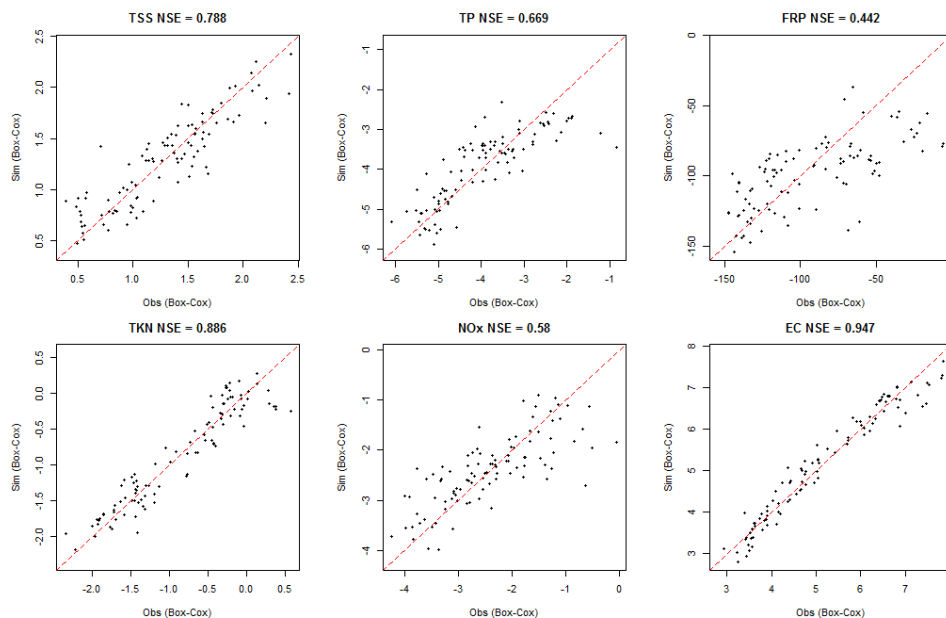
254 **Table 1. Comparison of model performance for all records and only the above-LOR records for**
 255 **each constituent.**

256

257 When simulating the site-level mean concentrations, the spatio-temporal models generally show good
 258 abilities to capture variability across sites for all constituents (Fig. 3). The highest model performance
 259 is for EC (explaining 94.7% of spatial variability) and lowest performance is for FRP (explaining
 260 44.2% spatial variability). The relative abilities of models to represent spatial variability in different



261 constituents are generally consistent with their capacities to capture spatio-temporal variability (Table
262 1).



263

264 **Figure 3. Model fit for site-level mean concentration at the 102 calibration sites, for the selected**
265 **six constituents, in Box-Cox transformed space. The NSE for each constituent is also show and**
266 **dashed red lines show the 1:1 lines.**

267 3.2 Model sensitivity to calibration sites and periods

268 This section presents model sensitivity to different calibration sites and periods of record (as detailed in
269 Sect. 2.4). Note that in these evaluations, the FRP model is not a focus due to the poor model
270 performance observed in Sect. 3.1.

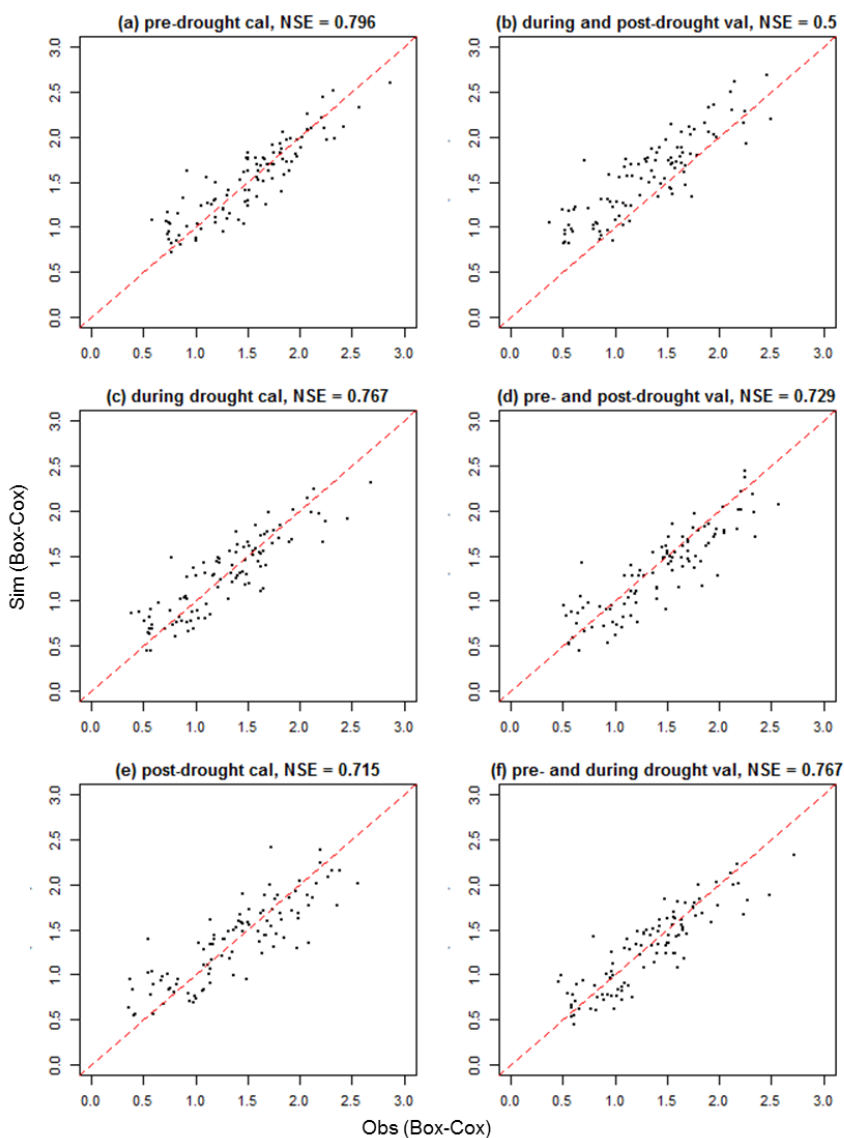
271 We first compare the performance of each spatio-temporal model fitted with the full dataset with those
272 obtained from the five corresponding “partial” models that were calibrated to only 80% of the
273 monitoring sites. Across constituents, the calibration performances obtained from the full dataset are
274 comparable with the five models calibrated with 80% of the sites (calibration dataset). In addition, each
275 pair of calibration and validation performance is highly consistent. In either comparison, the
276 corresponding differences in NSE are within 0.1 (Table 2, see Figs. S1 to S6 in the Supplementary
277 Material for detailed fitting plots for the partial calibration/validation). These suggest that the spatio-
278 temporal model performance are highly robust and remain unaffected by the choice of calibration sites.



279 **Table 2. Comparison of model performances (as NSE) of the full model (Column 2) and the five**
280 **partial models (Columns 3 to 7) with each calibrated to 80% randomly selected monitoring sites.**
281 **In Columns 3 to 7, the top row showing calibration performance and the bottom row showing**
282 **the validation performance (i.e. at the 20% sites that were not used for calibration).**
283

284 The performance of the full model for each constituent is also compared with that of the three models
285 calibrated to the pre-, during and post-drought periods. In general, we observe consistent performance
286 for each constituent, across calibrations to the three periods of contrasting hydrological conditions
287 (Table 3, see Figs. S7 to S12 in the Supplementary Material for detailed model fittings). One notable
288 common pattern is that the performance for calibration and validation is more consistent for the
289 drought period than either the pre- and post-drought periods. However, this is most likely explained by
290 relative sizes of the calibration data sets, which are 3, 13 and 5 years for the pre-, during and post-
291 drought periods respectively. Of all constituents (excluding FRP), TSS shows greater differences in
292 model performances across periods – especially when comparing the pre-drought calibration with its
293 validation. Fig. 4 shows the corresponding TSS model fit as represented by the site-level mean
294 concentrations for the three calibration/validation datasets. Notably, when calibrated to the pre-drought
295 period and validated on both the during- and post-drought periods, the model over-estimates a majority
296 of the data (Fig. 4 (b)); and when calibrated to the during-drought period, it slightly under-estimates
297 pre- and post-drought period TSS (Fig. 4 (d)).

298 **Table 3. Comparison of model performances (as NSE) of the full model and the three models**
299 **that were calibrated to the pre-drought (1994-1996), drought (1997-2009) and the post-drought**
300 **(2010-2014) periods. For each of the models, the calibration performance is shown on the top**
301 **row and the validation performance (i.e. over the periods that were not used for calibration) is**
302 **shown on the bottom row.**
303



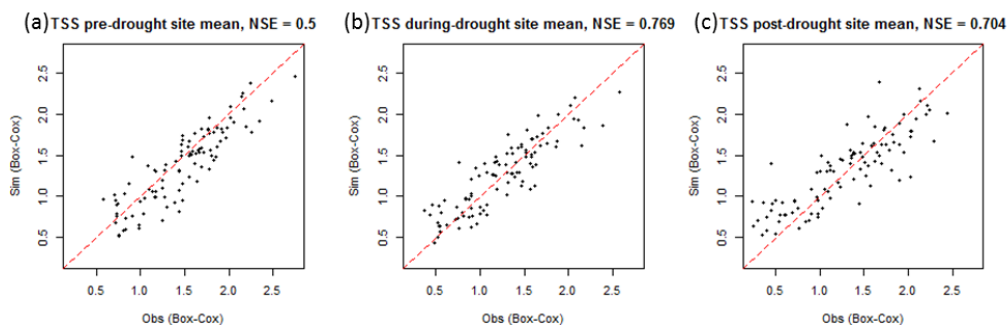
304
305
306
307
308
309
310
311

Figure 4. Comparison of the TSS model performance, as the simulated against observed site-level mean concentrations in Box-Cox transformed space. The left column shows calibration performance for the model calibrated to the pre-drought (1994-1996), drought (1997-2009) and the post-drought (2010-2014) periods, respectively; the right column shows the corresponding validation performance for each period. See Sect. 2.4 for details of the calibration and validation approach.

312 The potential impacts of drought on TSS dynamics are further illustrated with the performance of the
313 full spatio-temporal model over the pre-, during and post-drought periods (Fig. 5). Both the during-
314 and post-drought periods have consistently good performances, while the model underestimates the



315 majority of sites for the pre-drought period. This is consistent with Fig. 4 in suggesting a systematic
316 decrease in TSS concentration since the drought. The better performance of the full model during and
317 after drought (Fig. 5) can be a results of calibration period of the full spatio-temporal model – between
318 1994 and 2014 – which was dominated by the during- and post-drought periods; consequently, the full
319 spatio-temporal model can be largely defined by observed TSS dynamics during and after the drought.
320 In summary, Figs. 4 and 5 suggest that since the drought, TSS concentrations experienced a large-
321 scale downward shift compared to the pre-drought period, under otherwise identical spatial and
322 temporal conditions. Such a shift indicates changes in the relationships between TSS and its key
323 spatial and temporal controls since the start of the drought. Some possible causes are further discussed
324 in Sect. 4.3.



325

326 **Figure 5. Comparison of the performance of the full spatio-temporal TSS model across a) pre-**
327 **drought (1994-1996), b) during drought (1997-2009) and c) post-drought (2010-2014) periods, as**
328 **represented by the simulated against observed site-level mean concentrations in Box-Cox**
329 **transformed space.**

330 4. Discussion

331 4.1 Implications for statistical water quality modelling

332 Our spatial-temporal water quality models are able to capture the majority of observed variability across
333 the 102 sampling locations in Victoria (Sect. 3.1); the model performances also allow us to explore some
334 limitations of the modelling framework. The greatest limiting factor for model performance seems to be
335 when high proportions of LOR data are present. As shown in Fig. 2 and Table 1, model performance is
336 best for TKN and EC, where proportions of below-LOR records are low. For constituents where the
337 LOR records occupy greater proportions of the entire dataset, we observe poorer model performances
338 (e.g. FRP). As illustrated in Fig. 2, the FRP calibration data have a clear left-truncation pattern resulted



339 from removing a large proportion of below-LOR data. This substantially increased the degrees of
340 skewness and discontinuity of the data, essentially violating the assumption of linear modelling of
341 continuous data, and thus limiting the performance of the spatio-temporal model. It is worth noting that
342 in this study, since we modelled spatial and temporal variabilities in an integrated manner, the model
343 may compensate representation of the individual components of spatial and temporal variability to
344 improve fitting to the overall variability during calibration. Consequently, in this spatio-temporal
345 modelling framework, large presence of below-LOR data can limit the accurate representation of both
346 variability components.

347 Figure 2 highlights another possible influence on model performance, which is a combination of our
348 inability to analyse low concentrations and the limited resolution of these low-concentration
349 measurements due to heavy transformation in data processing. This is evidenced by visually inspecting
350 the fittings which show distinct “categorical” behaviour for low concentrations for some constituents.
351 This “categorical” issue impacts the six constituents to different extents, ranking from the strongest as:
352 FRP, TSS, TP, NO_x, TKN and EC – a ranking that is broadly aligned with the degree of lacking model
353 performance for these constituents. Similar to the below-LOR records, when these categorical values
354 are present in large proportions of the full records (e.g. TSS and FRP), they can also violate the linear
355 model assumptions and cause performance deterioration. This issue could be overcome by alternative
356 model structures that explicitly account for truncated data. For example, Wang and Robertson (2011)
357 and Zhao et al. (2016) illustrated an approach to resolving the discontinuity of the likelihood estimation
358 in modelling fitting to data with presence of zero values, which can be potentially extended to improve
359 fitting for the categorical levels at low concentrations.

360 In addition, our current models are empirical relationships which are likely unable to represent complex
361 biogeochemical processes. For example, performances for FRP and NO_x might be limited because: 1)
362 the linear model structure can over-simplify constituent dynamics due to biogeochemical processes that
363 are often highly non-linear; 2) the model may not include parameters that can adequately represent
364 relevant biogeochemical processes (due to the lack of these data). To better capture changes in reactive
365 constituents, greater consideration of and data representing biogeochemical processes may be required
366 to address nutrient cycling including denitrification, ammonification and mineralisation (Granger et al.,



367 2010). Therefore, possible ways to improve the statistical modelling of non-conservative constituents
368 are: 1) alternative non-linear statistical model structures; or 2) inclusion of parameters to better represent
369 biogeochemical processes.

370 Lastly, it is worth noting that our results are presented in the transformed scale for which the spatio-
371 temporal models were developed and the statistical assumptions hold (see details on data transformation
372 in Sect. 2.2). Model performance is heavily affected when simulated model outputs are back-
373 transformed to the measurement scale (see Figs. S13 in the Supplementary Information). However, our
374 models are very useful in representing and predicting proportional changes in concentrations, which
375 adds important information for assessing and managing catchment water quality. For example, an
376 increase of 1 mg L⁻¹ in suspended solids would be alarming in pristine streams and/or periods of good
377 water quality, while having much less impact on highly polluted conditions. The transformed models
378 developed in this study can help managers to understand these proportional changes to identify critical
379 locations and periods of key water quality concerns.

380 **4.2 Implications for water quality monitoring programs**

381 Within the current spatio-temporal models, water quality temporal variability is based on monthly
382 monitoring data. This suggests potential opportunities to further strengthen the model capacity to
383 explain temporal variability by utilizing data with higher temporal resolution. This approach can be
384 supported by recent developments that significantly improved the accessibility of high frequency water
385 quality monitoring data (Bende-Michl and Hairsine, 2010; Outram et al., 2014; Lannergård et al.,
386 2019; Pellerin et al., 2016). Another potential development is to use remote sensing data to augment low
387 frequency sampled data with higher frequency remotely sensed estimates e.g. for sediments and
388 nutrients (Glasgow et al., 2004; Ritchie et al., 2003). Alternatively, where high frequency data are lacking
389 for the target constituent, high frequency proxy data could also be utilized to enhance the understanding
390 obtained from low frequency samples. For example, turbidity can be used as surrogate for sediments
391 and nutrients (Schilling et al., 2017; Robertson et al., 2018; Lannergård et al., 2019). Currently,
392 continuous turbidity data are available from Australia state agencies, such as the Victorian Water Quality
393 Monitoring Network database (Department of Environment Land Water and Planning Victoria, 2016)
394 and the NSW Water information database (WaterNSW, 2018), and collated at national level in the



395 Bureau of Meteorology's Water Data Online portal (Bureau of Meteorology, 2019). These datasets may
396 have great potential to enhance the temporal resolutions of records for other key water quality
397 constituents (e.g. nutrients and sediments).

398 Changes in land management over time (e.g. tillage, fertiliser application, irrigation) are currently not
399 considered as predictors of water quality temporal variability. This is due to a lack of availability and/or
400 inconsistency of available data. However, changes in land use management practices can occur over
401 short time periods, which can lead to increases in pollutant sources and changes to runoff generation
402 processes (e.g. Tang et al., 2005; DeFries and Eshleman, 2004; Smith et al., 2013). Therefore, model
403 performance can potentially be further improved by increased capacities in the monitoring of temporal
404 patterns of land management.

405 **4.3 Potential impacts of long-term drought on water quality dynamics**

406 Results of model calibration and validation to different time periods suggest a systematic decrease in
407 TSS concentrations since the prolonged drought, in comparison with the pre-drought period under the
408 same spatial and temporal conditions. Such a shift is not observed for any other five constituents
409 analysed (nutrients and salts) (Sect. 3.2).

410 In the literature, impacts of the Millennium Drought on the hydrology and runoff regimes of south-
411 eastern Australia are well understood (van Dijk et al., 2013; Leblanc et al., 2012; Saft et al., 2015).
412 However, less is known about how this significant and prolonged drought event has impacted water
413 quality (Bond et al., 2008). Previous studies on other drought events around the world mainly focused
414 on changes in water quality as responses to the reduced streamflow during drought. For examples,
415 reduction in sediment levels have been reported during drought, due to lower erosion from the
416 contributing catchment and lower rates of solid transport associated with reduced flows (Murdoch et al.,
417 2000; Caruso, 2002). At a more local scale, increasing sediment concentrations during drought have also
418 been observed in streams adjacent to land with high densities of livestock and bushland, which both
419 constantly contribute to sediment load during drought, leading to elevated concentrations due to lower
420 dilution rate (Caruso, 2002). Similarly to sediments, the impact of droughts on stream nutrient and salt
421 concentrations were also commonly understood as responses to reduced runoff generation and



422 streamflow. Nutrient concentrations typically decrease during droughts in catchments with no
423 significant point-source pollution (Mosley, 2015), as nutrient leaching and overland flow are reduced
424 (Caruso, 2002). In contrast, catchments with significant point-source pollution generally experience
425 water quality deterioration during drought due to reduced dilution (van Vliet and Zwolsman,
426 2008; Mosley, 2015). For salinity, concentration often increases during drought with reduced dilution
427 and increased evaporation (Caruso, 2002), particularly for catchments that are more influenced by saline
428 groundwater input where drought can increase the relative contribution of saline groundwater input
429 (Costelloe et al., 2005).

430 However, our findings highlight other possible pathways on how drought can affect stream water
431 quality. The results suggest that the prolonged drought induced changes in sediment dynamics i.e.
432 changes of relationships between sediments and its predictors (Figs. 4 and 5). In contrast to sediments,
433 our models for nutrients and salts maintain consistent performance for different drought and non-drought
434 periods, suggesting no clear shifts in dynamics. A few studies have also reported changes in the
435 concentration-discharge relationships for sediments and nutrients. Specifically, these relationships
436 changed from high- to low-flow conditions (Zhang, 2018; Moatar et al., 2017), as well as from drought
437 to the recovery period (Burt et al., 2015). However, effects of extended multi-year droughts on the
438 concentration-discharge relationships are less explored. Furthermore, there is also a lack of
439 comprehensive assessments on the change of relationships between water quality and other relevant
440 controls (e.g. water temperature, land cover etc.) during extended drought over large geographical
441 regions. Our findings highlight great opportunities to use this dataset to further investigate the impacts
442 of prolonged droughts on water quality dynamics, especially the changes in relationships between TSS
443 and each of its key controls across multiple catchments.

444 In addition, we acknowledge that our ability to represent the pre- and post-drought conditions in this
445 study may be limited by the record length, since only 2 years of pre-drought and 4 years of post-drought
446 data were available. Once longer records build up, they will enable us to update our understanding of
447 the impact of this prolonged drought. We would be also able to conduct more sophisticated
448 investigations, such as comparing the impacts of long-term droughts versus individual dry and wet years.
449 Addressing these research questions are particularly important in a changing climate that will be



450 characterized by lower streamflows and possibly a shift towards more intermittent flows in many parts
451 of the world (Saft et al., 2015;Chiew et al., 2014;Ukkola et al., 2015).

452 **5. Conclusions**

453 Using long-term stream water quality data collected from 102 sites in south-eastern Australia, we
454 developed a Bayesian hierarchical statistical model to analyse the spatio-temporal variabilities in six
455 key water quality constituents: TSS, TP, FRP, TKN, NO_x and EC. The spatio-temporal models are
456 capable of predicting future water quality changes in non-monitored locations under similar conditions
457 to the historical period we investigated. A notable shift in TSS dynamics is observed since the extended
458 drought in the study region, which highlights potential oppourtunities for further research to better
459 understand the impact of this significant drought event on water quality.

460 Despite the promising performance of these models, the results also illustrate areas of further
461 improvement, both in the modelling framework but also in the monitoring of water quality. In improving
462 the modelling framework, alternative statistical approaches could be considered to reduce the impact of
463 below detection limit and low concentration data on model performance. In addition, the models could
464 be extended to take into account some key biogeochemical processes to better represent spatial-temporal
465 variability in non-conservative constituents (e.g., FRP or NO_x). To further enhance the performance of
466 the current models, we recommend that future water quality monitoring programs be enhanced with: 1)
467 collection and assimilation of high-frequency sampling data to enhance the temporal resolution of water
468 quality data; and 2) more frequent monitoring of changes in land use intensity and management to be
469 able to include these parameters in the model. These improvements will be very helpful to operational
470 catchment management and mitigation.

471 **Data availability**

472 All data used in this study were extracted from public domain. All stream water quality data were
473 extracted from the Victorian Water Measurement Information System (via <http://data.water.vic.gov.au/>,
474 provided by the Department of Environment Land Water and Planning Victoria). The catchments
475 corresponding to these water quality monitoring sites were delineated using the Geofabric tool provided
476 by the Bureau of Meteorology, via <ftp://ftp.bom.gov.au/anon/home/geofabric/>. We have listed the



477 sources of all other data for the spatial and temporal predictors of our models in Tables S1 and S2 in the
478 Supplementary Materials.

479 **Author contribution**

480 All authors contributed to the conceptualization the models and the design of methodology. A. Lintern
481 and S. Liu contributed to the data curation. D.Guo carried out the formal analyses, visualization and
482 validation. J.A. Webb, D. Ryu, U. Bende-Michl and A.W. Western contributed to the funding
483 acquisition. D. Guo, A. Lintern, J.A. Webb, D. Ryu, S. Liu and A.W. Western contributed to the
484 investigation. D. Guo carried out project administration and coding to run the experiments. J.A. Webb,
485 D. Ryu, and A.W. Western contributed to the supervision. D.Guo prepared the manuscript with
486 contributions from all co-authors.

487 **Competing interests**

488 The authors declare that they have no conflict of interest.

489 **Acknowledgement**

490 Australian Research Council and the Victorian Environment Protection Authority, the Victorian
491 Department of Environment, Land Water and Planning, the Bureau of Meteorology and the Queensland
492 Department of Natural Resources, Mines and Energy provided funding for this project through the
493 linkage program (LP140100495). The authors would also like to thank Matthew Johnson, Louise
494 Sullivan, Hannah Sleeth and Jie Jian, for their assistance in the compilation and analysis of data. All
495 water quality data used for this project can be found on: Water Measurement Information System
496 (<http://data.water.vic.gov.au/monitoring.htm>). Sources of other data are provided in Tables S1 and S2
497 of the Supplementary Materials.

498



499 References

- 500 Abbaspour, K. C., Rouholahnejad, E., Vaghefi, S., Srinivasan, R., Yang, H., and Kløve, B.: A
501 continental-scale hydrology and water quality model for Europe: Calibration and uncertainty of a high-
502 resolution large-scale SWAT model, *Journal of Hydrology*, 524, 733-752,
503 <https://doi.org/10.1016/j.jhydrol.2015.03.027>, 2015.
- 504 Ai, L., Shi, Z. H., Yin, W., and Huang, X.: Spatial and seasonal patterns in stream water contamination
505 across mountainous watersheds: Linkage with landscape characteristics, *Journal of Hydrology*, 523,
506 398-408, <https://doi.org/10.1016/j.jhydrol.2015.01.082>, 2015.
- 507 Akaike, H.: A new look at the statistical model identification, *IEEE transactions on automatic control*,
508 19, 716-723, 1974.
- 509 Australian Water Technologies: Victorian water quality monitoring network and state biological
510 monitoring programme manual of procedures, Australian Water Technologies, 68 Ricketts Rd, Mt
511 Waverley VIC 3149, 1999.
- 512 Bende-Michl, U., and Hairsine, P. B.: A systematic approach to choosing an automated nutrient analyser
513 for river monitoring, *Journal of Environmental Monitoring*, 12, 127-134, 2010.
- 514 Bengraïne, K., and Marhaba, T. F.: Using principal component analysis to monitor spatial and temporal
515 changes in water quality, *Journal of Hazardous Materials*, 100, 179-195, [https://doi.org/10.1016/S0304-](https://doi.org/10.1016/S0304-3894(03)00104-3)
516 [3894\(03\)00104-3](https://doi.org/10.1016/S0304-3894(03)00104-3), 2003.
- 517 Bond, N. R., Lake, P. S., and Arthington, A. H.: The impacts of drought on freshwater ecosystems: an
518 Australian perspective, *Hydrobiologia*, 600, 3-16, 10.1007/s10750-008-9326-z, 2008.
- 519 Borsuk, M. E., Higdon, D., Stow, C. A., and Reckhow, K. H.: A Bayesian hierarchical model to predict
520 benthic oxygen demand from organic matter loading in estuaries and coastal zones, *Ecological*
521 *Modelling*, 143, 165-181, [https://doi.org/10.1016/S0304-3800\(01\)00328-3](https://doi.org/10.1016/S0304-3800(01)00328-3), 2001.
- 522 Bureau of Meteorology: Geofabric V2 2012.
- 523 Bureau of Meteorology: Water Data Online, 2019.
- 524 Bureau of Rural Sciences: 2005/06 Land use of Australia, version 4. . 2010.
- 525 Burt, T. P., Worrall, F., Howden, N. J. K., and Anderson, M. G.: Shifts in discharge-concentration
526 relationships as a small catchment recover from severe drought, *Hydrological Processes*, 29, 498-507,
527 10.1002/hyp.10169, 2015.
- 528 Caruso, B. S.: Temporal and spatial patterns of extreme low flows and effects on stream ecosystems in
529 Otago, New Zealand, *Journal of Hydrology*, 257, 115-133, [https://doi.org/10.1016/S0022-](https://doi.org/10.1016/S0022-1694(01)00546-7)
530 [1694\(01\)00546-7](https://doi.org/10.1016/S0022-1694(01)00546-7), 2002.
- 531 Chang, H.: Spatial analysis of water quality trends in the Han River basin, South Korea, *Water Research*,
532 42, 3285-3304, <https://doi.org/10.1016/j.watres.2008.04.006>, 2008.
- 533 Chiew, F. H. S., Potter, N. J., Vaze, J., Petheram, C., Zhang, L., Teng, J., and Post, D. A.: Observed
534 hydrologic non-stationarity in far south-eastern Australia: implications for modelling and prediction,
535 *Stochastic Environmental Research and Risk Assessment*, 28, 3-15, 10.1007/s00477-013-0755-5, 2014.
- 536 Clark, J. S.: Why environmental scientists are becoming Bayesians, *Ecology Letters*, 8, 2-14,
537 doi:10.1111/j.1461-0248.2004.00702.x, 2005.
- 538 Costelloe, J. F., Grayson, R. B., McMahon, T. A., and Argent, R. M.: Spatial and temporal variability
539 of water salinity in an ephemeral, arid-zone river, central Australia, *Hydrological Processes*, 19, 3147-
540 3166, 10.1002/hyp.5837, 2005.
- 541 DeFries, R., and Eshleman, K. N.: Land-use change and hydrologic processes: a major focus for the
542 future, *Hydrological Processes*, 18, 2183-2186, doi:10.1002/hyp.5584, 2004.
- 543 Department of Environment Land Water and Planning Victoria: Victorian water measurement
544 information system. . 2016.



- 545 Eidenshink, J. C.: The 1990 Conterminous U.S. AVHRR Data Set, Photogrammetric Engineering and
546 Remote Sensing, 58, 1992.
- 547 Frost, A. J., Ramchurn, A., and Smith, A.: The bureau's operational AWRA landscape (AWRA-L)
548 Model, Bureau of Meteorology, 2016.
- 549 Fu, B., Merritt, W. S., Croke, B. F. W., Weber, T., and Jakeman, A. J.: A review of catchment-scale
550 water quality and erosion models and a synthesis of future prospects, Environmental Modelling &
551 Software, <https://doi.org/10.1016/j.envsoft.2018.12.008>, 2018.
- 552 Geoscience Australia: Dams and water storages. . 2004.
- 553 Geoscience Australia: Environmental Attributes Dataset. 2011.
- 554 Glasgow, H. B., Burkholder, J. M., Reed, R. E., Lewitus, A. J., and Kleinman, J. E.: Real-time remote
555 monitoring of water quality: a review of current applications, and advancements in sensor, telemetry,
556 and computing technologies, Journal of Experimental Marine Biology and Ecology, 300, 409-448,
557 <https://doi.org/10.1016/j.jembe.2004.02.022>, 2004.
- 558 Granger, S. J., Bol, R., Anthony, S., Owens, P. N., White, S. M., and Haygarth, P. M.: Chapter 3 -
559 Towards a Holistic Classification of Diffuse Agricultural Water Pollution from Intensively Managed
560 Grasslands on Heavy Soils, in: Advances in Agronomy, Academic Press, 83-115, 2010.
- 561 Guo, D., Lintern, A., Webb, J. A., Ryu, D., Liu, S., Bende-Michl, U., Leahy, P., Wilson, P., and Western,
562 A. W.: Key Factors Affecting Temporal Variability in Stream Water Quality, Water Resources Research,
563 55, 112-129, 10.1029/2018wr023370, 2019.
- 564 Hrachowitz, M., Benettin, P., van Breukelen, B. M., Fovet, O., Howden, N. J. K., Ruiz, L., van der
565 Velde, Y., and Wade, A. J.: Transit times—the link between hydrology and water quality at the
566 catchment scale, Wiley Interdisciplinary Reviews: Water, 3, 629-657, doi:10.1002/wat2.1155, 2016.
- 567 Kaushal, S. S., Mayer, P. M., Vidon, P. G., Smith, R. M., Pennino, M. J., Newcomer, T. A., Duan, S.,
568 Welty, C., and Belt, K. T.: Land Use and Climate Variability Amplify Carbon, Nutrient, and
569 Contaminant Pulses: A Review with Management Implications, JAWRA Journal of the American Water
570 Resources Association, 50, 585-614, doi:10.1111/jawr.12204, 2014.
- 571 Kingsford, R. T., Walker, K. F., Lester, R. E., Young, W. J., Fairweather, P. G., Sammut, J., and Geddes,
572 M. C.: A Ramsar wetland in crisis – the Coorong, Lower Lakes and Murray Mouth, Australia, Marine
573 and Freshwater Research, 62, 255-265, <https://doi.org/10.1071/MF09315>, 2011.
- 574 Kisi, O., and Parmar, K. S.: Application of least square support vector machine and multivariate adaptive
575 regression spline models in long term prediction of river water pollution, Journal of Hydrology, 534,
576 104-112, <https://doi.org/10.1016/j.jhydrol.2015.12.014>, 2016.
- 577 Kurunç, A., Yürekli, K., and Çevik, O.: Performance of two stochastic approaches for forecasting water
578 quality and streamflow data from Yeşilirmak River, Turkey, Environmental Modelling & Software, 20,
579 1195-1200, <https://doi.org/10.1016/j.envsoft.2004.11.001>, 2005.
- 580 Lannergård, E. E., Ledesma, J. L., Fölster, J., and Futter, M. N.: An evaluation of high frequency
581 turbidity as a proxy for riverine total phosphorus concentrations, Science of the Total Environment, 651,
582 103-113, 2019.
- 583 Leblanc, M., Tweed, S., Van Dijk, A., and Timbal, B.: A review of historic and future hydrological
584 changes in the Murray-Darling Basin, Global and Planetary Change, 80-81, 226-246,
585 <https://doi.org/10.1016/j.gloplacha.2011.10.012>, 2012.
- 586 Lintern, A., Webb, J. A., Ryu, D., Liu, S., Bende-Michl, U., Waters, D., Leahy, P., Wilson, P., and
587 Western, A. W.: Key factors influencing differences in stream water quality across space, Wiley
588 Interdisciplinary Reviews: Water, 5, e1260, doi:10.1002/wat2.1260, 2018a.
- 589 Lintern, A., Webb, J. A., Ryu, D., Liu, S., Waters, D., Leahy, P., Bende-Michl, U., and Western, A. W.:
590 What Are the Key Catchment Characteristics Affecting Spatial Differences in Riverine Water Quality?,
591 Water Resources Research, doi:10.1029/2017WR022172, 2018b.



- 592 May, R., Dandy, G., and Maier, H.: Review of input variable selection methods for artificial neural
593 networks, in: Artificial neural networks-methodological advances and biomedical applications, InTech,
594 2011.
- 595 Meybeck, M., and Helmer, R.: The quality of rivers: From pristine stage to global pollution,
596 Palaeogeography, Palaeoclimatology, Palaeoecology, 75, 283-309, [https://doi.org/10.1016/0031-](https://doi.org/10.1016/0031-0182(89)90191-0)
597 [0182\(89\)90191-0](https://doi.org/10.1016/0031-0182(89)90191-0), 1989.
- 598 Moatar, F., Abbott, B. W., Minaudo, C., Curie, F., and Pinay, G.: Elemental properties, hydrology, and
599 biology interact to shape concentration-discharge curves for carbon, nutrients, sediment, and major ions,
600 Water Resources Research, 53, 1270-1287, 10.1002/2016wr019635, 2017.
- 601 Mosley, L. M.: Drought impacts on the water quality of freshwater systems; review and integration,
602 Earth-Science Reviews, 140, 203-214, <https://doi.org/10.1016/j.earscirev.2014.11.010>, 2015.
- 603 Murdoch, P. S., Baron, J. S., and Miller, T. L.: POTENTIAL EFFECTS OF CLIMATE CHANGE ON
604 SURFACE-WATER QUALITY IN NORTH AMERICA1, JAWRA Journal of the American Water
605 Resources Association, 36, 347-366, 10.1111/j.1752-1688.2000.tb04273.x, 2000.
- 606 NASA LP DAAC: MOD13A3: MODIS/Terra Vegetation Indices Monthly L3 Global 1km V005. 2017.
- 607 Outram, F. N., Lloyd, C. E. M., Jonczyk, J., Benskin, C. M. H., Grant, F., Perks, M. T., Deasy, C., Burke,
608 S. P., Collins, A. L., Freer, J., Haygarth, P. M., Hiscock, K. M., Johnes, P. J., and Lovett, A. L.: High-
609 frequency monitoring of nitrogen and phosphorus response in three rural catchments to the end of the
610 2011–2012 drought in England, Hydrol. Earth Syst. Sci., 18, 3429-3448, 10.5194/hess-18-3429-2014,
611 2014.
- 612 Ouyang, W., Hao, F., Skidmore, A. K., and Toxopeus, A. G.: Soil erosion and sediment yield and their
613 relationships with vegetation cover in upper stream of the Yellow River, Science of The Total
614 Environment, 409, 396-403, <https://doi.org/10.1016/j.scitotenv.2010.10.020>, 2010.
- 615 Parmar, K. S., and Bhardwaj, R.: Statistical, time series, and fractal analysis of full stretch of river
616 Yamuna (India) for water quality management, Environmental Science and Pollution Research, 22, 397-
617 414, 10.1007/s11356-014-3346-1, 2015.
- 618 Pellerin, B. A., Stauffer, B. A., Young, D. A., Sullivan, D. J., Bricker, S. B., Walbridge, M. R., Clyde
619 Jr., G. A., and Shaw, D. M.: Emerging Tools for Continuous Nutrient Monitoring Networks: Sensors
620 Advancing Science and Water Resources Protection, JAWRA Journal of the American Water Resources
621 Association, 52, 993-1008, 10.1111/1752-1688.12386, 2016.
- 622 Qin, B., Zhu, G., Gao, G., Zhang, Y., Li, W., Paerl, H. W., and Carmichael, W. W.: A Drinking Water
623 Crisis in Lake Taihu, China: Linkage to Climatic Variability and Lake Management, Environmental
624 Management, 45, 105-112, 10.1007/s00267-009-9393-6, 2010.
- 625 Raupach, M., Briggs, P., Haverd, V., King, E., Paget, M., and Trudinger, C.: Australian water
626 availability project (AWAP): CSIRO marine and atmospheric research component: final report for phase
627 3, 67, 2009.
- 628 Raupach, M., Briggs, P., Haverd, V., King, E., Paget, M., and Trudinger, C.: Australian Water
629 Availability Project. CSIRO Marine and Atmospheric Research, Canberra, Australia., 2012.
- 630 Ritchie, J. C., Zimba, P. V., and Everitt, J. H.: Remote Sensing Techniques to Assess Water Quality,
631 Photogrammetric Engineering & Remote Sensing, 69, 695-704, 10.14358/PERS.69.6.695, 2003.
- 632 Robertson, D. M., Hubbard, L. E., Lorenz, D. L., and Sullivan, D. J.: A surrogate regression approach
633 for computing continuous loads for the tributary nutrient and sediment monitoring program on the Great
634 Lakes, Journal of Great Lakes Research, 44, 26-42, <https://doi.org/10.1016/j.jglr.2017.10.003>, 2018.
- 635 Saft, M., Western, A. W., Zhang, L., Peel, M. C., and Potter, N. J.: The influence of multiyear drought
636 on the annual rainfall-runoff relationship: An Australian perspective, Water Resources Research, 51,
637 2444-2463, doi:10.1002/2014WR015348, 2015.



- 638 Saft, M., Peel, M. C., Western, A. W., and Zhang, L.: Predicting shifts in rainfall-runoff partitioning
639 during multiyear drought: Roles of dry period and catchment characteristics, *Water Resources Research*,
640 52, 9290-9305, doi:10.1002/2016WR019525, 2016.
- 641 Schilling, K. E., Kim, S.-W., and Jones, C. S.: Use of water quality surrogates to estimate total
642 phosphorus concentrations in Iowa rivers, *Journal of Hydrology: Regional Studies*, 12, 111-121,
643 <https://doi.org/10.1016/j.ejrh.2017.04.006>, 2017.
- 644 Schwarz, G.: Estimating the dimension of a model, *The annals of statistics*, 6, 461-464, 1978.
- 645 Smith, A. P., Western, A. W., and Hannah, M. C.: Linking water quality trends with land use
646 intensification in dairy farming catchments, *Journal of Hydrology*, 476, 1-12, 2013.
- 647 Stan Development Team: RStan: the R interface to Stan. R package version 2.18.1, 2018.
- 648 Tang, Z., Engel, B. A., Pijanowski, B. C., and Lim, K. J.: Forecasting land use change and its
649 environmental impact at a watershed scale, *Journal of Environmental Management*, 76, 35-45,
650 <https://doi.org/10.1016/j.jenvman.2005.01.006>, 2005.
- 651 Terrestrial Ecosystem Research Network: Soil and landscape grid of Australia. 2016.
- 652 Trambly, Y., Ouarda, T. B. M. J., St-Hilaire, A., and Poulin, J.: Regional estimation of extreme
653 suspended sediment concentrations using watershed characteristics, *Journal of Hydrology*, 380, 305-
654 317, <https://doi.org/10.1016/j.jhydrol.2009.11.006>, 2010.
- 655 Ukkola, A. M., Prentice, I. C., Keenan, T. F., van Dijk, A. I. J. M., Viney, N. R., Myneni, Ranga B., and
656 Bi, J.: Reduced streamflow in water-stressed climates consistent with CO₂ effects on vegetation, *Nature*
657 *Climate Change*, 6, 75, 10.1038/nclimate2831
- 658 <https://www.nature.com/articles/nclimate2831#supplementary-information>, 2015.
- 659 van Dijk, A. I. J. M., Beck, H. E., Crosbie, R. S., de Jeu, R. A. M., Liu, Y. Y., Podger, G. M., Timbal,
660 B., and Viney, N. R.: The Millennium Drought in southeast Australia (2001–2009): Natural and human
661 causes and implications for water resources, ecosystems, economy, and society, *Water Resources*
662 *Research*, 49, 1040-1057, 10.1002/wrcr.20123, 2013.
- 663 van Vliet, M. T. H., and Zwolsman, J. J. G.: Impact of summer droughts on the water quality of the
664 Meuse river, *Journal of Hydrology*, 353, 1-17, <https://doi.org/10.1016/j.jhydrol.2008.01.001>, 2008.
- 665 Victorian water measurement information system: <http://data.water.vic.gov.au/monitoring.htm>, 2016.
- 666 Vörösmarty, C. J., McIntyre, P. B., Gessner, M. O., Dudgeon, D., Prusevich, A., Green, P., Glidden, S.,
667 Bunn, S. E., Sullivan, C. A., Liermann, C. R., and Davies, P. M.: Global threats to human water security
668 and river biodiversity, *Nature*, 467, 555, 10.1038/nature09440
- 669 <https://www.nature.com/articles/nature09440#supplementary-information>, 2010.
- 670 Wang, Q. J., and Robertson, D. E.: Multisite probabilistic forecasting of seasonal flows for streams with
671 zero value occurrences, *Water Resources Research*, 47, 10.1029/2010wr009333, 2011.
- 672 Wang, Q. J., Shrestha, D. L., Robertson, D. E., and Pokhrel, P.: A log-sinh transformation for data
673 normalization and variance stabilization, *Water Resources Research*, 48, doi:10.1029/2011WR010973,
674 2012.
- 675 Real-time water data: <https://realtimedata.waternsw.com.au/>, access: 12/07/2018, 2018.
- 676 Webb, J. A., and King, L. E.: A Bayesian hierarchical trend analysis finds strong evidence for large-
677 scale temporal declines in stream ecological condition around Melbourne, Australia, *Ecography*, 32,
678 215-225, doi:10.1111/j.1600-0587.2008.05686.x, 2009.
- 679 Whitworth, K. L., Baldwin, D. S., and Kerr, J. L.: Drought, floods and water quality: Drivers of a severe
680 hypoxic blackwater event in a major river system (the southern Murray–Darling Basin, Australia),
681 *Journal of Hydrology*, 450-451, 190-198, <https://doi.org/10.1016/j.jhydrol.2012.04.057>, 2012.



- 682 Zhang, Q.: Synthesis of nutrient and sediment export patterns in the Chesapeake Bay watershed:
683 Complex and non-stationary concentration-discharge relationships, *Science of The Total Environment*,
684 618, 1268-1283, <https://doi.org/10.1016/j.scitotenv.2017.09.221>, 2018.
- 685 Zhao, T., Schepen, A., and Wang, Q. J.: Ensemble forecasting of sub-seasonal to seasonal streamflow
686 by a Bayesian joint probability modelling approach, *Journal of Hydrology*, 541, 839-849,
687 <https://doi.org/10.1016/j.jhydrol.2016.07.040>, 2016.
- 688
- 689



690 **Tables**

691 **Table 1. Comparison of model performance for all records and only the above-LOR records for**
 692 **each constituent.**

Constituent	Above-LOR records only	All records
TSS	0.225	0.397
TP	0.433	0.445
FRP	-1.920	0.199
TKN	0.658	0.630
NO _x	0.216	0.382
EC	0.907	0.886

693

694 **Table 2. Comparison of model performances (as NSE) of the full model (Column 2) and the five**
 695 **partial models (Columns 3 to 7) with each calibrated to 80% randomly selected monitoring sites.**
 696 **In Columns 3 to 7, the top row showing calibration performance and the bottom row showing**
 697 **the validation performance (i.e. at the 20% sites that were not used for calibration).**

Constituent	Full model	80% sites split 1	80% sites split 2	80% sites split 3	80% sites split 4	80% sites split 5
TSS	0.397	0.406	0.431	0.390	0.428	0.423
		0.348	0.441	0.443	0.446	0.434
TP	0.445	0.440	0.422	0.440	0.472	0.456
		0.386	0.444	0.454	0.449	0.444
FRP	0.199	0.141	0.219	0.244	0.216	0.177
		0.041	0.350	0.337	0.356	0.344
TKN	0.630	0.664	0.643	0.630	0.658	0.669
		0.639	0.589	0.581	0.584	0.587
NO _x	0.382	0.410	0.464	0.438	0.476	0.466
		0.419	0.593	0.603	0.597	0.597
EC	0.886	0.895	0.894	0.875	0.900	0.892
		0.796	0.828	0.837	0.828	0.826

698

699 **Table 3. Comparison of model performances (as NSE) of the full model and the three models**
 700 **that were calibrated to the pre-drought (1994-1996), drought (1997-2009) and the post-drought**
 701 **(2010-2014) periods. For each of the models, the calibration performance is shown on the top**
 702 **row and the validation performance (i.e. over the periods that were not used for calibration) is**
 703 **shown on the bottom row.**

Constituent	Full model	Pre-drought calibration	During drought calibration	Post-drought calibration
TSS	0.397	0.495	0.399	0.499
		0.208	0.402	0.390
TP	0.445	0.477	0.438	0.525
		0.421	0.474	0.411
FRP	0.199	-1.336	0.187	0.204
		-1.406	0.197	0.024
TKN	0.630	0.649	0.650	0.711
		0.566	0.648	0.610
NO _x	0.382	0.443	0.426	0.509
		0.394	0.471	0.393
EC	0.886	0.854	0.901	0.901
		0.887	0.873	0.884

704